# Two lanthanide-based metal-organic frameworks for highly efficient adsorption and removal of fluoride ion from water

Aiqing Ma[a#], Ke Fei[#b*], Jing Jiang[b], Qiaoyu Yuan[b], Zhidong Luo[a], Jianqiang Liu[a*], Abhinav Kumar[c]

### *Batch adsorption experiments*

In order to determine the adsorption capacity of the two lanthanide-based MOFs for fluoride ion, batch fluoride adsorption experiments were carried out. Typically, 30 mg of adsorbent (**1** or **2**) was added to 15 mL of the fluoride solutions (400, 200, 100, 50, 25 and 12.5 ppm, respectively) in a 50 mL conical-bottom polypropylene tubes. The mixture was immediately placed in a vapor-bath constant temperature oscillator at 250 rpm for a certain time at room temperature. After filtration, both initial and the remaining fluoride concentrations were measured using fluoride-selective electrode. Total ionic strength adjustment buffer (TISAB) was used to maintain accuracy in the readings. 10 mL of TISAB was added to 10 mL sample solutions and standards. All measurements were carried out at 25°C, and the adsorption capacity ($q_e$, mg $g^{-1}$) of the adsorbents for fluoride was calculated according to the following equation:

$$q_e = \frac{(C_0 - C_e)V}{m} \quad (1)$$

Where $C_0$ and $C_e$ represent the initial and equilibrium fluride concentrations (mg $L^{-1}$), respectively, $V$ represents the volume of solution (L), and $m$ represents the mass of adsorbent (g) used.

### *Adsorption kinetics and thermodynamics*

The kinetic experiments were established by adding 30 mg of the adsorbents (**1** or **2**) into 15 mL of the fluoride solution with the initial concentration of fluoride 12.5 ppm. The mixtures were placed in a vapor-bathing constant temperature oscillator under constant shaking at a speed of 250 rpm, and maintained at the temperature of 25 °C. The response on fluoride-selective electrode was recorded at intervals to monitor the progress of the adsorption.

To study the thermodynamics mechanism, the effect of contact temperature on the adsorption of fluoride onto the adsorbents (**1** or **2**) were monitored by adding 30 mg adsorbents into 15 mL of the fluoride solution (from 12.5 to 400 ppm) at shaking

temperature of 25 ºC, 35 ºC and 45 ºC.

**pseudo-second-order kinetic equation**

$$\frac{t}{q_t} = \frac{1}{k_2 q_e^2} + \frac{t}{q_e}$$

where $k_2$ is the rate constant of the pseudo-second-order adsorption (g $mg^{-1}$ $min^{-1}$), $q_t$ and $q_e$ represent the amount of fluoride adsorbed at time $t$ and equilibrium (mg $g^{-1}$), respectively.

**Langmuir equation**

$$\frac{C_e}{q_e} = \frac{1}{q_m K_L} + \frac{C_e}{q_m}$$

where $q_m$ is the maximum adsorption capacity (mg $g^{-1}$), $C_e$ is the equilibrium concentration of remaining fluoride in the solution (mg $L^{-1}$), and $K_L$ is the Langmuir adsorption constant (L $mg^{-1}$)

**Gibbs free energy (Δ*G*) equation**

$$\Delta G = -RT \ln K \quad (4)$$

Where Δ*G* is the free energy change of adsorption (kJ $mol^{-1}$), *K* is the thermodynamic equilibrium constant equal to $q_m \times K_L$ of Langmuir isotherm.

**Description of structure in 1**

Each SBU consists of two equivalent $Ce^{3+}$ (Fig. 1) and each $Ce^{3+}$ is coordinated by nine oxygen atoms to result in a CeO9 unit, where two O atoms come from coordinated water molecules, two O atoms come from coordinated nitrate ion and the other five O atoms are from carboxylic oxygen. The nine O atoms around $Ce^{3+}$ are arranged in a distorted tri-capped triangular prism (Fig. S1). The ligands have two coordination modes of $\mu_2$-$\eta^2$-$\eta^1$ and$\mu_2$-$\eta^1$-$\eta^1$.

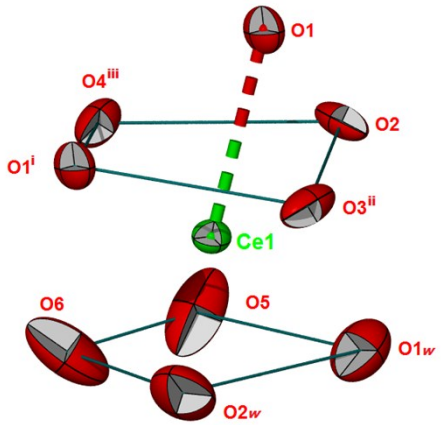


Fig. S1 The distorted tri-capped triangular prism of CeO9 in **1**.

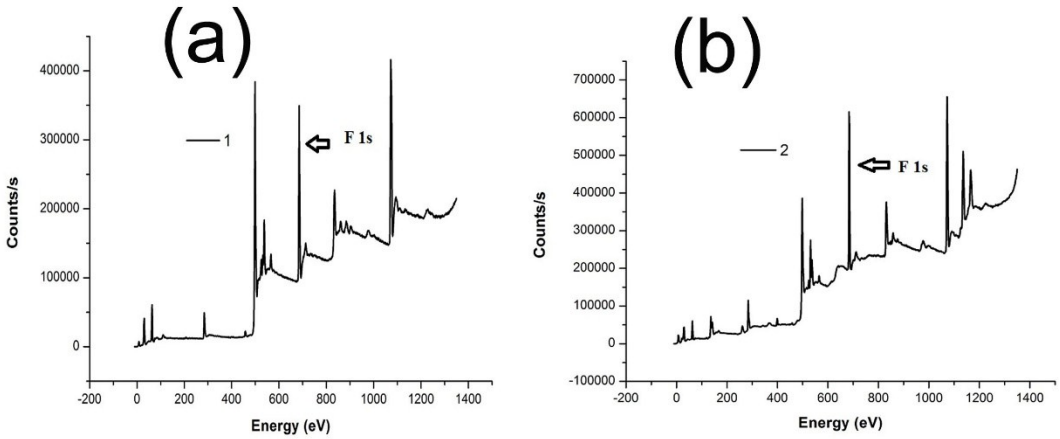


Fig. S2. (a) F1s XPS spectra of **1**@$F^-$ and (b) F1s XPS spectra of **2**@$F^-$

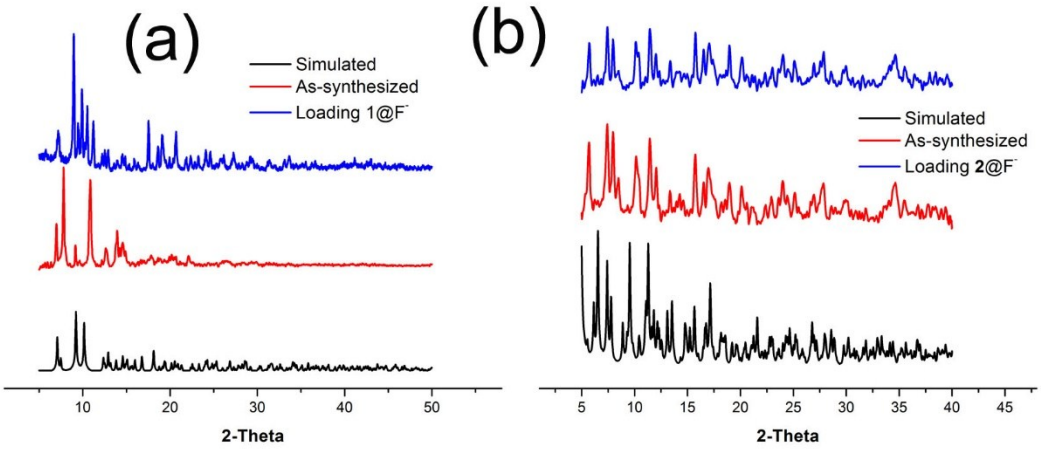


Fig S3 (a) Powder X-ray diffraction (PXRD) patterns of simulated (black) and as-synthesized **1** (red), and activated **1**@$F^-$ (blue). (b) Powder X-ray diffraction (PXRD) patterns of simulated

(black) and as-synthesized **2** (red), and activated **2**@$F^-$ (blue).

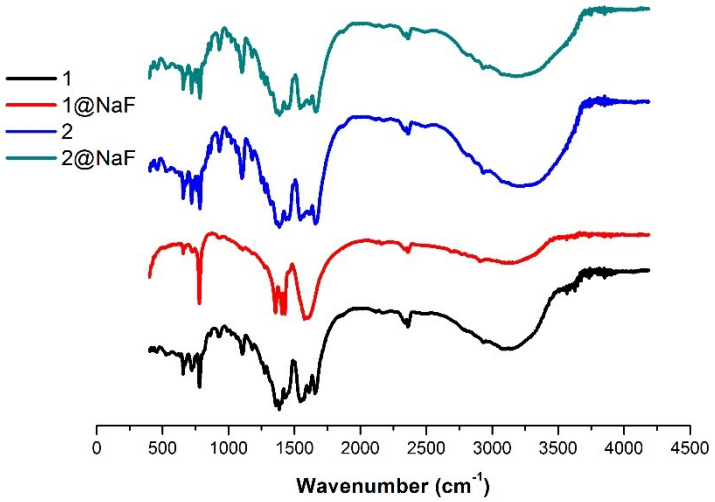


Fig. S4 View of the IR spectra of **1**, **1**@$F^-$, **2** and **2**@$F^-$.

Stability Analysis

Thermogravimetric analysis (TGA) for **1** shows a weight loss of 30.43 % between 30 and 310°C (Fig. S5), which corresponds to the loss of two free DMF molecules and two coordinated $H_2O$ moelcules (calcd: 31.08 %). Upon further heating, a weight loss corresponds to the release of the organic L1 ligand and the coordinated $NO_3^-$, and then the collapse of the framework.

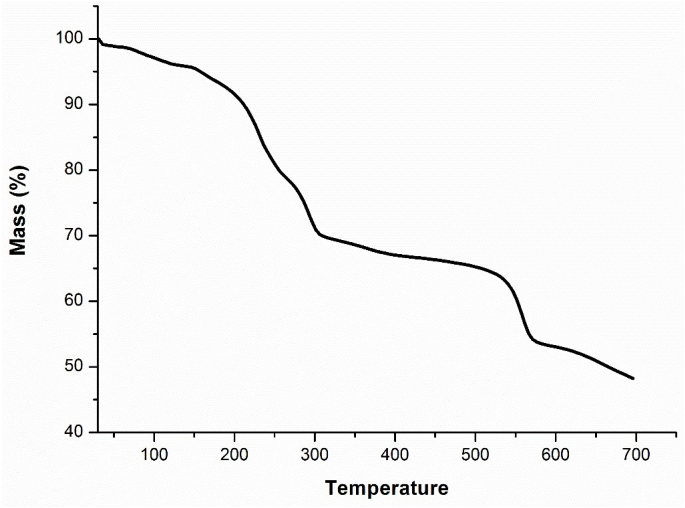


Fig. S5 curve of TGA in **1**.

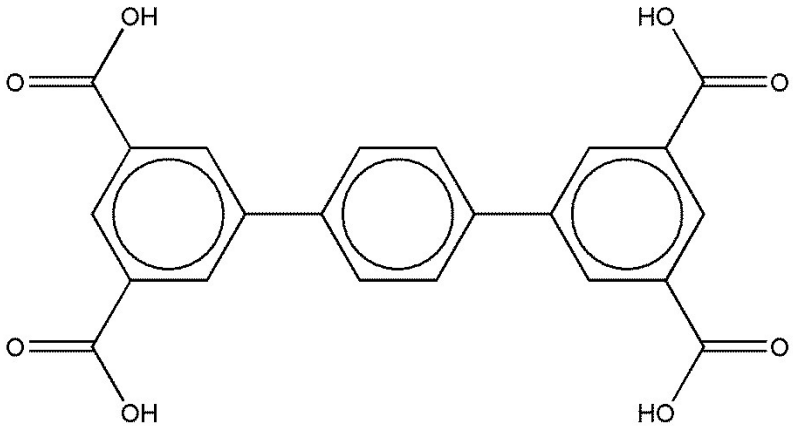


$H_4L1$

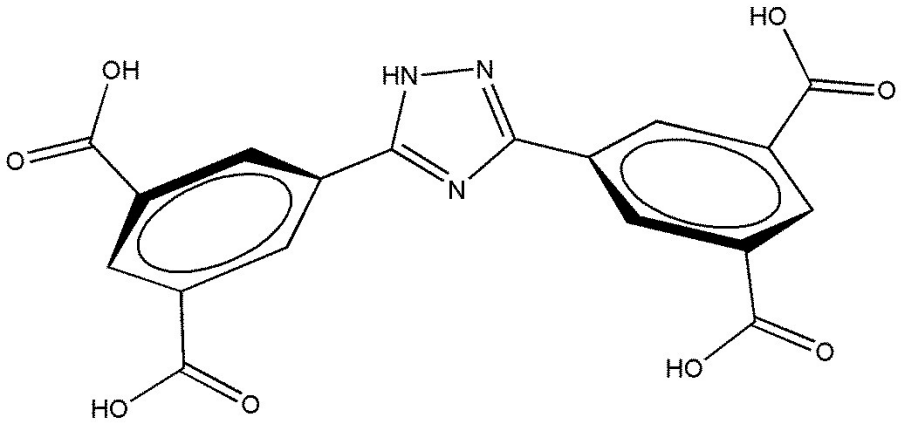


$H_4L2$

Scheme S1 view of the skeleton of ligands in this work.

Table S1 Textural properties, the pseudo-second-order kinetics rate constants ($k_2$) with the amount of fluoride adsorbed at equilibrium ($q_e$) and the correlation coefficients (R) of the two adsorbents.

| No. | $q_e$ | $k_2$ | $R$ |
|---|---|---|---|
| | mg.g$^{1}$ | g.mg$^{-1}$ | min$^{-1}$ |
| **1** | 5.66 | 1.79 | 1 |
| **2** | 3.77 | 0.37 | 0.9999 |

**Table S2.** Crystal data and structure refinement information for compound **1**

| Parameter | **1** |
|---|---|
| Formula | $C_{11}H_9CeNO_9$ |
| Formula weight | 439.31 |
| Crystal system | Monoclinic |
| Space group | $C_2/c$ |
| Crystal color | colorless |
| *a,* [Å] | 25.5147(15) |
| *b,* [Å] | 13.4137(8) |
| *c,* [Å] | 14.6329(9) |
| α, [°] | 90.00 |
| β, [°] | 101.9661(9) |
| γ, [°] | 90.00 |
| *V*, Å $^3$ | 4899.2(5) |
| *Z* | 4 |
| $\rho_{calcd}$, g/cm$^3$ | 1.588 |
| μ, mm$^{-1}$ | 1.915 |
| *F*(000) | 2336 |
| θ Range, deg | 2.34–27.29 |
| Reflection collected | 16658/ 6341 |
| Goodness-of-fit on $F^2$ | 1.039 |
| $R_1$, $wR_2(I> 2\sigma(I))^*$ | 0.0562, 0.1506 |
| $R_1$, $wR_2$ (all data)$^{**}$ | 0.0806, 0.1698 |

* $R = \sum(F_o - F_c)/\sum(F_o)$, ** $wR_2 = \{\sum[w(F_o^2 - F_c^2)^2]/\sum(F_o^2)^2\}^{1/2}$.

**Table S3** Selected bond distances (Å) and angles (°) of **1**

| | | | |
|---|---|---|---|
| Ce(1)-O(3) | 2.433(7) | Ce(1)-O(1W) | 2.442(8) |
| Ce(1)-O(1)#1 | 2.450(6) | Ce(1)-O(4) | 2.457(6) |
| Ce(1)-O(2W) | 2.475(8) | Ce(1)-O(2) | 2.508(6) |

| | | | |
|---|---|---|---|
| Ce(1)-O(5) | 2.619(9) | Ce(1)-O(6) | 2.763(7) |
| O(3)-Ce(1)-O(4) | 131.7(2) | O(3)-Ce(1)-O(5) | 151.7(3) |
| O(2W)-Ce(1)-O(2) | 146.6(3) | O(1)-Ce(1)-O(2) | 122.0(2) |

Symmetry codes: #1: -x, y, -z+1/2.